Preliminary design of aerospace linear actuator housings

Fabien Hospital, Marc Budinger, Aurelien Reysset, Jean-Charles Maré

PRELIMINARY DESIGN OF AEROSPACE LINEAR ACTUATOR HOUSINGS

Fabien Hospital, Marc Budinger, Aurélien Reysset, Jean-Charles Maré

Université de Toulouse; INSA, UPS, Mines Albi, ISAE; ICA (Institut Clément Ader)
135, avenue de Rangueil, F-31077 Toulouse, France

ABSTRACT

Purpose - Aerospace actuation systems are currently tending to become more electrical and fluid free. Methodologies and models already exist for designing the mechanical and electrical components but the actuator housing design is still sketchy. This paper proposes preliminary design models of actuator housing that enable various geometries to be compared without requiring detailed knowledge of the actuator components.

Design/methodology/Approach - The approach is dedicated to linear actuators, the most common in aerospace. With special attention paid to mechanical resistance to the vibratory environment, simplified geometries are proposed to facilitate the generation of an equivalent formal development. The vibratory environment imposes the sizing of the actuator housing. Depending on the expected level of details and vibration boundary conditions, three levels of modeling have been created.

Practical Implications - This approach is applied to a comparison of six standard designs of linear actuator geometries after validation of the consistency of the different models. Early conclusions can be drawn and may lead to design perspectives for the definition of actuator architecture and the optimization of the design.

Finding - This article shows that the vibrations induced by aircraft environment are not design drivers for conventional hydraulic actuators but can be an issue for new electromechanical actuators. The weight of the latter can be optimized through a judicious choice of the diameter of the housing.

Originality/value - This article has demonstrated the importance of the vibratory environment in the design of linear actuator housing, especially for electro-mechanical actuators with important strokes. Developed analytical models can be used for the overall design and optimization of these new aerospace actuators.

Keywords electro-mechanical actuator, housing, preliminary design, vibration, Modelica, modeling

Article Classification Research paper

Introduction

The current technical developments in air transport call for cheaper, safer and more environmentally friendly systems, along with ever shorter times to market and an increasing demand for quality and advanced functions. This trend is propagating to actuation for landing gears and flight controls, which are often the main secondary power consumers. Power-by-wire (PbW) actuation, in particular, is an attractive way to remove centralized hydraulic power networks, by distributing power through electric wires to the power users. PbW actuators have recently been introduced in the new generation of commercial aircraft (Van den Bossche, 2001) (Todeschi, 2010), in replacement of conventional servo-hydraulic ones (SHA). For example, the Boeing B787 integrates EMA spoiler actuation, as does the Airbus A380 (backup only), and electrical brakes. Space launchers are following the same trend for thrust vector control (TVC) as illustrated by various NASA projects (Cowan and Weir, 1993) and, more recently, by the European VEGA project (Dée, Vanthuyne and Alexandre, 2010) .

EMAs are currently being carefully considered by aircraft makers and equipment suppliers as they completely remove hydraulics, even at the actuator level. Unfortunately, EMAs are still heavier and bulkier than their SHA counterparts. Besides their direct impact on the total aircraft mass, they make the actuator more sensitive to the vibratory environment and require special attention during preliminary sizing and assessment (Grand and Valembois, 2004) (EUROCAE, 2005). In particular, the EMA housing often appears as a major contributor to the overall actuator mass (it may represent thirty to forty percent of the mass) and also impacts integration and actuator optimization.

In the early phases of an actuation project, only a few design parameters are available but major technical decisions have to be taken (INCOSE, 2004). However, designers still lack simple and expressive (i.e. with an adequate level of detail) models that suit the needs of preliminary design. In practice, the housing is generally first defined through pure geometrical considerations to integrate the EMA parts while keeping within the allocated housing. Resistance to vibration is assessed a posteriori during real vibration tests. It is clear that the housing sizing is still poorly addressed in common practice for preliminary design. The definition of actuator housing is a complex task because it depends on the geometries of other parts and their relative arrangement.

The present work aims to offer efficient, simple tools for fast and easy preliminary design of housings for linear actuators, considering their resistance to vibrations. It will complete the models for the design of power transmission components (electric motors, reducers, bearings, etc.) that are being developed to provide an integrated preliminary design process with associated in-house CAE tools (Liscouet et al., 2011) (Budinger et al., 2012).

Section 2 starts with a review of the state of the art in actuator housing design. Then, it introduces the different topologies of linear actuators, which leads to a proposal for three generic representations of the actuator housing geometry. It ends by reviewing the sizing stresses and addressing the state of the art in vibration studies. In section 0, the analytical models related to the first two representations are derived using Rayleigh theory, which allows the mechanical stress versus the geometry to be studied in a single model. Section 4 deals with the third representation. In this section, the transfer matrix theory enables a modular approach which is implemented as a dedicated tool with the Modelica simulation language. Section 5 starts by comparing the accuracy of the three representations. The second part of this section is dedicated to the assessment of each method on real cases, considering six common geometries of servo-hydraulic, electro-hydrostatic and electromechanical actuators. Section 6 uses the results obtained to create surrogate models of housings sized to withstand vibration-induced stress. This proposal finally provides an automated way of linking the overall actuator mass to the actuator requirements at the very beginning of a project.

STATE OF THE ART ON DESIGN DRIVERS AND MODELLING METHODS FOR LINEAR ACTUATOR HOUSINGS

Various candidate topologies can meet the requirements of a given actuator. As far as linear actuators are concerned, the most common design involves a screw/nut to transform rotation into translation. Although the actuator housing depends strongly on how the internal components are arranged, it can be represented by a simplified model for vibration studies, as described in section 2.1. However, the actuator housing also has to meet its own requirements and design constraints. This particularly concerns its resistance to the static and dynamic stresses that propagate from the actuated load through various load paths within the actuator, as explained in section 2.2. The stresses induced by the vibratory environment are addressed in section 2.3.

TOPOLOGICAL ARCHITECTURES OF LINEAR ACTUATOR HOUSINGS IN AEROSPACE

The major mechanical components used in aerospace EMAs, as seen Figure 1 on several examples of applications, are summarised in (Budinger et al., 2012). Different classes of generic components are pointed out, such as brushless motors (cylindrical or annular), mechanical power transmission and transformation (e.g. gearboxes or nut-screw), mechanical bearings and joints (e.g. thrust bearings or spherical end bearings) and possibly mechanical power management (e.g. clutches or brakes). It is observed that among all the candidate topologies of components arrangements, the parallel axis design is widely used. That is why it will be considered in the following sections.

As presented in (Karam and Maré, 2006), standard assemblies of in-line linear actuators and their housings are generally similar. Four generic designs can be associated with the transformation of rotation into translation: rotating nut or translating nut, standard or inverted screw. A sample of aerospace linear actuator cross sections is represented in Figure 1.

FIGURE 1 Different architectures and scales of standard EMA compared with a hydraulic actuator

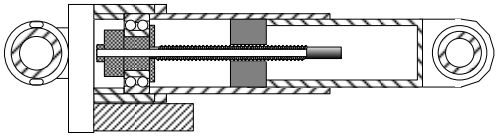

Long and wide EMA type, main stage TVC of VEGA launcher (Dée, Vanthuyne and Alexandre, 2010) (Vanthuyne, 2009)

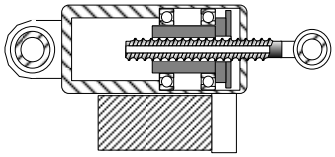

Translating screw type EMA of F-18 (Jensen, Jenney and Dawson, 2000)

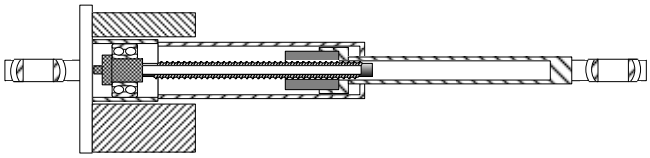

Long and thin EMA type nose landing gear actuator (Chevalier, Grac and Liegois, 2010)

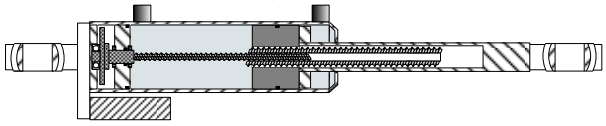

Hybrid type EBMA of A400M landing gear doors (Chevalier, Grac and Liegois, 2010)

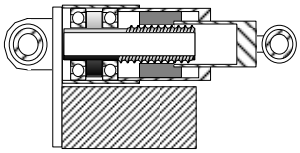

Short EMA type spoiler (Davis, 1984)

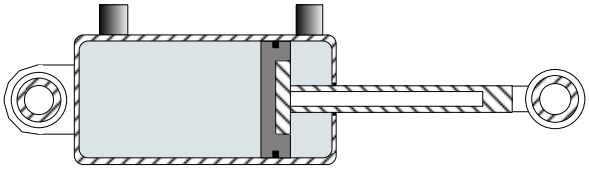

Hydraulic type SHA, Airbus A320 Aileron

In each case, the shape of the actuator housing can be modelled with the same geometry. For this reason and similarly to the hydraulic actuator, modelling the linear actuator housing is proposed with different levels of details as follows:

- In the simplest representation of
- Figure **2** - a, the rod and the body are considered as a single hollow cylinder while an equivalent mass is introduced as a global lumped inertial effect coming from the mechanical transmission components.
- In the middle representation of
- Figure **2** - b, the rod is dissociated from the housing, each body being considered as a single cylinder.
- In the more realistic representation of
- Figure **2** - c, the rod and the body are made of an assembly of cylinders whose masses are representative of the actuator integrated components.

For any model, the mass of the cylinder is distributed assuming a constant density.

This proposal enables analytical approaches to be used that take advantage of beam theory. In the particular case of "hybrid" actuators (Maré, 2011), that is to say EMA coupled with hydraulic actuators in the same physical unit, the mass of the fluid is added into the model. All the vibration studies were conducted on totally deployed actuators to perform the sizing in the most critical situation in terms of mechanical stresses.

FIGURE 2 PROPOSED MODELS OF A STANDARD LINEAR ACTUATOR HOUSING

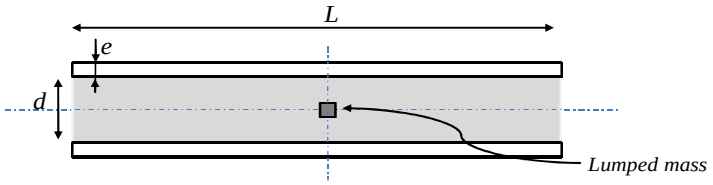

A – Single-body model

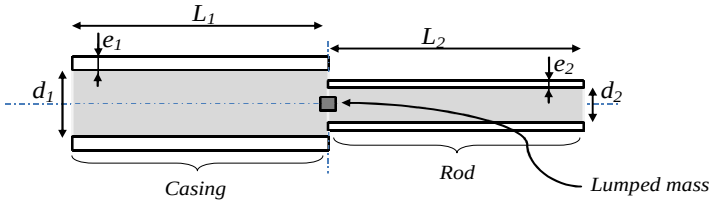

B – Two-body model

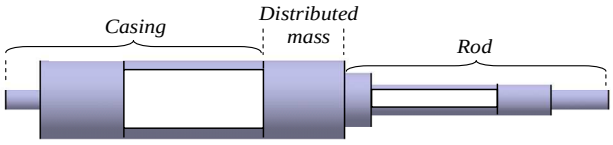

C - Realistic model

HOUSING FUNCTIONS AND MAIN DESIGN DRIVERS

The main functions of the housing of actuators are the following (Boubet, 1998): Integration (joints and bearings) of the actuator components, Sealing towards the outside for lubricant, Sealing towards the inside for humidity or dust (breath phenomena), Thermal dissipation of energy losses towards the environment, Protection of internal components against shocks and vibrations, Anchorage to the airframe.

From a purely mechanical point of view, the design of the EMA housing has to focus on the elementary forces acting on the housing, which can be divided into two categories: the mechanical stresses induced by the

power transmission to the load, which are low frequency (static), and the vibratory induced stresses, which are very dynamic:

- Static load sizing generated by:
  - Tensile/compressive/buckling forces that are transmitted through the rod to the nut and the screw, then to the thrust bearing and finally to the housing. The high number of cycles generally requires the fatigue limits of materials to be taken into account.
  - Shearing and bending stresses that are due to the masses of components and friction torques in spherical bearings or anchorage points.
  - Torsion stresses induced by friction and reaction torques of motor / reducers / nut screw.
- Dynamic stress sizing generated by:
  - Transversal vibrations due to the vibratory environment which can generate important mechanical bending stresses.
  - Transient rotational, longitudinal and transversal loads (e.g. at stop-end).

The tensile/compressive/buckling stress is the most significant static load that the actuator receives. Other static loads are often considered as unimportant and stemming from parasitic efforts. The path of the various static or dynamic loads is represented for a generic actuator on *FIGURE 3*. It has to be noticed that spherical end-bearings can, in some cases, perform an anti-rotation function through the actuator's mechanical connections (making a gimbal link at the actuator mechanical interfaces).

FIGURE 3 LOADS PATH IN A GENERIC EMA

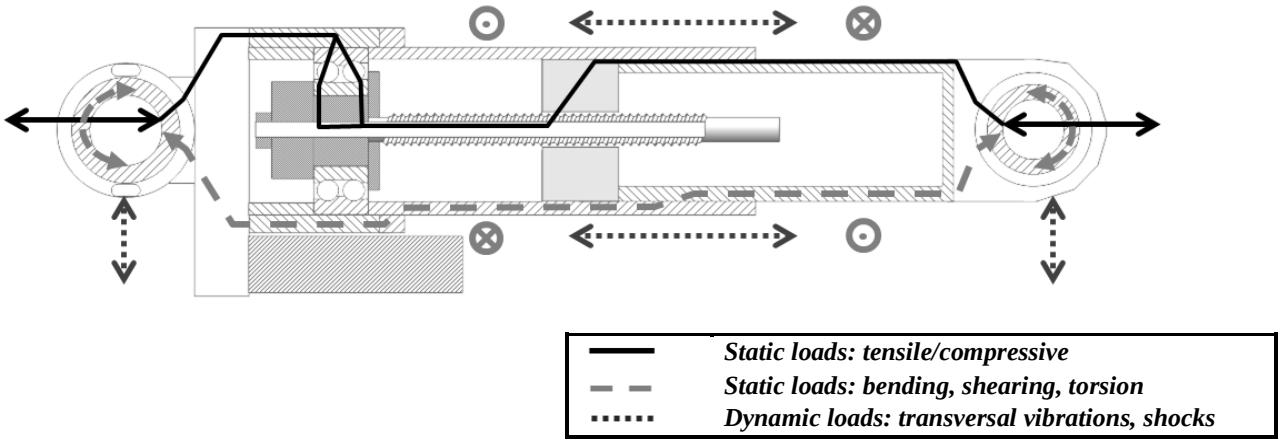

STATE OF THE ART OF MECHANICAL HOUSING DESIGN IN HARSH VIBRATORY ENVIRONMENT

Previous actuator studies and experiment feedback have shown that the stresses induced by the vibratory environment can be much more significant than "static" loading, especially for linear actuators that are very slender (slenderness λ=L/D, ratio of the extended length to the average diameter). For this reason, the state of the art focuses on the design of housings of mechanical structures in a harsh vibratory environment with special reference to aerospace.

Current methods for the design of housings in vibratory environments In the literature, few publications dealing with the design of housings are available. The most common methods used can be divided into two categories. On the one hand, empirical methods (Morgado, Branco and Infante, 2008) (Rebbechi, 1999) use experimental results for fatigue calculations. On the other hand, finite element methods (FEM) (Samuelson, Holm and Esping, 1991) (Topaç, Günal and Kuralay, 2009) detect numerically critical points in fixed

conditions and for a given geometry. However, it must be pointed out that the proposed methods also apply to housing geometries that are very different from the EMA geometries. Experimental methods are often used because they provide reliable results. Unfortunately, they only apply to particular geometries of existing hardware. Similarly, FEM studies also require the 3D geometry to be defined. In a model-based process, the preliminary design of an actuator should take advantage of fast definition of housings to meet the integration requirements and to assess the candidate concepts and topologies, without detailed knowledge of the housing geometry. As the above-mentioned approaches cannot meet this need, developing simple analytic methods is of great interest. Although these methods require marked simplifications, it will be shown below that they can provide useful predictions.

Aerospace vibratory environment simplification through sinus excitation In aerospace, the performance requirements concerning vibrations generally refer to the DO160E standard (EUROCAE, 2005), which considers two aspects: resistance to impact and crash, and resistance to vibrations. The test curves of vibratory levels versus frequency depend on the type of aircraft, the device location and the test category (standard, high level and short duration, robust). Two different excitations can be performed: sinusoidal test procedure or random test procedure with a given acceleration power spectral density. In this paper, a sinusoidal acceleration excitation within the [5 Hz, 2000 Hz] frequency range will be considered. The acceleration magnitude depends mainly on the location of the device on the aircraft and on the type of aircraft. In some cases, a power spectral density over a narrow frequency interval can be translated into an equivalent sinusoidal excitation.

ANALYTIC MODEL WITH RAYLEIGH THEORY

In this section, a linear hybrid EMA filled with oil will be assumed to be equivalent to the two simplified geometries of

FIGURE **2** - *A* and

FIGURE **2** - *B*:

- The single-body model composed of one hollow cylinder, of interior diameter *d*, thickness *e*, and length *L*, with spherical joint on its ends.
- The two-body model composed of two perfectly embedded hollow cylinders 1 and 2, each with a length *L/2;* d_1 / d_2 and e_1 / e_2 being the interior diameter and thickness of cylinders 1 and 2 respectively.

For these two geometries, two effects can be taken into account for the vibratory sizing of actuators: the inertial effect of the embedded mass of the power transmission mechanical components (especially the roller/screw) with a mass M_{comp} (

FIGURE **2**) and the inertial effect of the hydraulic fluid of density ρ_h.

MODELLING ASSUMPTIONS AND EQUIVALENT SYSTEM

The geometries of *FIGURE 1* or
FIGURE **2** can be seen as continuous structures with distributed mass and compliance effects with an infinite number of resonance modes. However, the magnitude of the displacements of the first natural frequency is generally higher than those of the other resonance modes. Consequently, as the maximum stress is proportional to displacement (Harris and Piersol, 2001), only the first mode will be studied here. The damped mass-spring system presented on

FIGURE 4 is the most usual way to study mechanical system vibrations through an equivalent lumped parameter model. In this scheme, the notations and assumptions are the following:

- u_0 the displacement of the system mass M_{eq} from its equilibrium position;
- K_{eq} the stiffness of the system (perfect spring with zero mass);
- C_{eq} the equivalent structural damping coefficient (perfect damper with zero mass);
- F the excitation force.

FIGURE 4 MASS SPRING SYSTEM WITH DAMPING

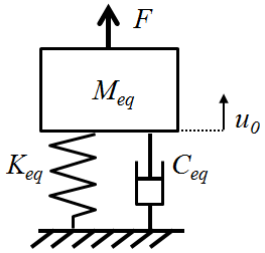

Newton's second law applied to the moving body enables the Laplace function between the displacement $u_0(t)$ and the excitation load $F(t)$ to be calculated:

$$\frac{u_0(p)}{F(p)} = \frac{1}{M_{eq}.p^2 + C_{eq}.p + K_{eq}} = \frac{1/K_{eq}}{p^2/\omega_n^2 + 2.\xi.p/\omega_n + 1} \quad (1)$$

Considering a sinusoidal excitation of the mass with a force of magnitude F_0 (which means $F(t)=F_0.sin(\omega t)$), the magnitude of the displacement becomes:

$$u_{0,\max} = \frac{1}{2\xi}.\frac{F_0}{K_{eq}} = \frac{Q.F_0}{K_{eq}} \quad where \quad \xi = \frac{C_{eq}}{2\sqrt{K_{eq}.M_{eq}}} \approx \frac{1}{2Q} \quad (2)$$

Tests performed on industrial prototypes show a wide range of practical values for the damping coefficient ξ or the equivalent mechanical quality coefficient Q. Experiments give typical values for Q between 10 and 50, depending on the application and boundary conditions. For structural dynamic models, in the absence of better information, it is normally acceptable to assume a value of $Q=30$ (Agency, 2007). A theoretical study carried out in the laboratory but not presented in this article, has shown that the quality coefficient depends strongly on test conditions, in particular on the excitation accelerations. This is due to nonlinear effects (e.g. contact compliance, dry friction, etc.). That is why particular attention should be paid to this coefficient.

MODELING PRINCIPLES

Wave equation The bending vibrations of a metallic tube can be studied using a beam model of the strength of materials. To establish the wave equation, an elementary volume of the beam is isolated, with cross-section S and second area moment I. The orthogonal and rotational displacements are noted u and Ψ respectively. The internal efforts are expressed as the bending moment T_f and to the shear force F_T respectively. The bending moment, shear force and rotation displacement are obtained by derivation of the orthogonal displacement.

Newton's second law applied to this elementary volume allows the wave equation to be written (Gerardin and Rixen, 1993) (Hatch, 2001). The solution is generally noted in complex variables, assuming a sinusoidal shape of the form:

$$U(x,t) = \mathrm{Re}\left[A(x).je^{-j\omega t}\right] \quad (3)$$

Thus, the differential equation of elastic wave propagation admits equation (6) as solution.

$$A(x) = a.\sin(kx) + b.\cos(kx) + c.\sinh(kx) + d.\cosh(kx) \quad (4)$$

where k is a coefficient depending on the pulsation and geometry and where a, b, c and d are parameters associated with the boundary conditions.

Single body model In the geometry of FIGURE 5, displacements $U(x,t)$ are written as a function of the displacement of the center of the beam ($U(0,t)=u_0(t)$). The boundary conditions allow the unknown coefficients *a, b, c* and *d* to be defined. Finally, the displacement expression is:

$$\forall x \in \left[-\frac{L}{2};\frac{L}{2}\right],\ U(x,t) = u_0(t).u(x) = u_0(t).\cos\left(\frac{\pi}{L}x\right) \qquad (5)$$

As exact expressions can quickly become too heavy to handle when the model has more than one body, it is possible and common to approximate the displacement with a polynomial function.

FIGURE 5 PARAMETERIZING THE SINGLE BODY MODEL DEFORMATION

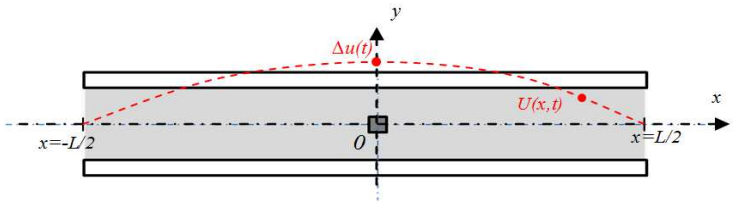

According to the Lagrangian approach, and considering the assumptions of part 3.2.1, M_{eq}, the equivalent mass and K_{eq} the equivalent stiffness can be calculated from the kinetic energy and the energy of elastic deformation (Gerardin and Rixen, 1993) (Lagrange, 1853). In the present case, if the inertial torque and the deformations due to shearing are neglected, the expressions become:

$$M_{eq} = \int \rho.S.u(x)^2\,dx \Rightarrow M_{eq} = \rho.S\frac{L}{2} \qquad (6)$$

$$K_{eq} = \int_{-L/2}^{+L/2} EI\left(\frac{\partial\Psi(x)}{\partial x}\right)^2 dx \Rightarrow K_{eq} = \frac{\pi^4}{2}\frac{EI}{L^3} \qquad (7)$$

where ρ is the housing density and L its length, the other parameters being described in section 3.2.1.

Bending vibration tests are performed by applying the same displacement to the beam anchorage points with a given acceleration magnitude. Thus the problem is similar to a fixed beam subjected to a given acceleration ($a(t)=a_0.sin(\omega t)$). By writing the equation of the total work, it is possible to extract the excitation force applied to the center of the beam *F(t):*

$$u_0(t).F(t) = \int_{-L/2}^{+L/2} a(t).\rho.S.U(x,t).dx \Rightarrow F_0 = a_0.\frac{2.\rho.S.L}{\pi} \qquad (8)$$

If the fluid effect and the mass of power transmission components are added, then expressions (6) and (8) become:

$$M_{eq} = \rho.S\frac{L}{2} + \rho_h.S_h\frac{L}{2} + M_{comp} \quad \Rightarrow F_0 = a_0.\left(\frac{2.\rho.S.L}{\pi} + \frac{2.\rho_h.S_h.L}{\pi} + M_{comp}\right) \qquad (9)$$

where S_h is the hydrostatic area and M_{comp} the components of mechanical transmission mass.

With mass and stiffness expressions, it is possible to calculate the first resonance frequency of the housing subjected to its own weight. At this resonance, the maximum deformation and the maximum stress under vibrations are thus expressed as a function of the acceleration magnitude, quality coefficient and housing geometry. The maximum stress is therefore linked to the resonance frequency. Materials, quality coefficient and acceleration amplitude depend on the testing conditions and on the excitation input.

Thus, σ_{max} maximum mechanical stress can be evaluated using:

$$\sigma_{max} = y_{max}.E.\left.\frac{\partial\psi}{\partial x}\right|_{x=0} = \left(\frac{d}{2}+e\right).E.\left(u_{0,max}.\left(\frac{\pi}{L}\right)^2\right) = \left(\frac{d}{2}+e\right).E.\left(\frac{Q.F_0}{K_{eq}}.\left(\frac{\pi}{L}\right)^2\right) \qquad (10)$$

where y_{max} is the position along the y axis on the section area in which the stress is calculated .

Two-body model In the geometry of FIGURE 6, displacements $U_i(x,t)$ are written as a function of the displacement of the center of the beam $\Delta u(t)$. Two hollow cylinders are assumed to represent the left hand side (cylinder 1 with displacement $U_1(x,t)$) and the right hand side (cylinder 2 with displacement $U_2(x,t)$) of the housing.

FIGURE 6 PARAMETERIZING THE TWO-BODY MODEL DEFORMATION

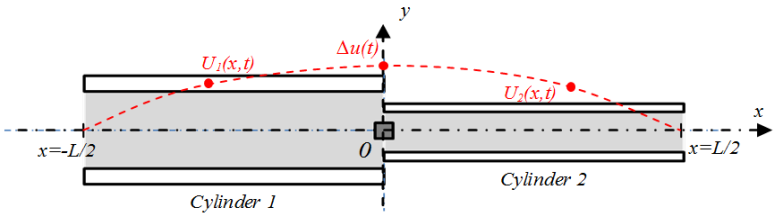

To simplify the development analysis, a polynomial approximation of the displacement of each side may be preferred to the exact sinusoidal expression. For the single body geometry, such an approximation gives results with a 4% error compared with the cosine beam shape of equation (5). In the two-body model, the displacement of each side is a function of x and the five constants a_i, b_i, c_i, d_i, e_i of the polynomial representation.

$$\forall i \in \{1,2\},\quad \forall \breve{x} = x/(L/2) \in [-1,1],\quad U_i(x,t) = \Delta u(t).u_i(x) = \Delta u(t).\left(a_i + b_i.\breve{x} + c_i.\breve{x}^2 + d_i.\breve{x}^3 + e_i.\breve{x}^4\right) \tag{11}$$

The boundary conditions define all the constants of polynomial expressions U_1 and U_2 except one. That is why the final expressions of deformations are parameterized by the remaining coefficient b.

$$\begin{cases} u_1(\breve{x}) = 1 + b.\breve{x} + \frac{3}{5}(b\text{-}br\text{-}r\text{-}1).\breve{x}^2 + (1\text{-}b\text{-}r\text{-}br).\breve{x}^3 + \frac{1}{5}(3\text{-}3b\text{-}2r\text{-}2br).\breve{x}^4 \\ u_2(\breve{x}) = 1 + b\breve{x} + \frac{3}{5r}(b\text{-}br\text{-}r\text{-}1).\breve{x}^2 + \frac{1}{r}(1\text{-}b\text{-}r\text{-}br).\breve{x}^3 + \frac{1}{5}(3 + 3b\text{-}\frac{2}{r} + \frac{2b}{r}).\breve{x}^4 \end{cases} \tag{12}$$

with $r=E_2I_2/(E_1I_1)$; E_1 , E_2 being the Young's modulus of the two housing cylinders; I_1 , I_2 the second area moments.

In the Lagrangian approach (Lagrange, 1853), the equivalent mass and the equivalent stiffness are expressed as a function of the unknown coefficient b. It is then possible to determine it by adding this coefficient in the unknowns of the Lagrangian of the system:

$$L(\Delta u, \Delta \dot{u}, b) = \frac{1}{2} M_{eq}(b).\Delta \dot{u}(t)^2 - \frac{1}{2} K_{eq}(b).\Delta u(t)^2 \tag{13}$$

In the case of sinusoidal displacement $u_0(t)$ at a pulsation ω, the Lagrange's equations become:

$$\begin{cases} M_{eq}\omega^2 - K_{eq} = 0 \\ \frac{\partial M_{eq}}{\partial b}\omega^2 - \frac{\partial K_{eq}}{\partial b} = 0 \end{cases} \tag{14}$$

which gives two equations with two unknowns: b and ω. The expressions for the coefficients α_i, β_i, γ_i are given in appendix A. M_{eq} and K_{eq} have the following form:

$$\begin{cases} M_{eq} = \alpha_1 b^2 + \beta_1 b + \gamma_1 \\ K_{eq} = \alpha_2 b^2 + \beta_2 b + \gamma_2 \end{cases}, with \begin{cases} \alpha_1, \beta_1, \gamma_1 = f(\rho_1, \rho_2, S_1, S_2, L, r) \\ \alpha_2, \beta_2, \gamma_2 = f(I_1, I_2, E_1, E_2, L, r) \end{cases} \quad (15)$$

Lagrange's equations can be written in a different way in order to solve the problem. And *b* is the solution of the quadratic equation that maximizes the displacement:

$$\begin{cases} \omega = \sqrt{\dfrac{\alpha_2 b^2 + \beta_2 b + \gamma_2}{\alpha_1 b^2 + \beta_1 b + \gamma_1}} \\ (\alpha_1\beta_2 - \alpha_2\beta_1)b^2 + (2\alpha_1\gamma_2 - 2\alpha_2\gamma_1)b + (\beta_1\gamma_2 - \beta_2\gamma_1) = 0 \end{cases} \quad (16)$$

As for the one-body model, the bending vibration consist in applying a given acceleration ($a(t)=a_0.sin(\omega t)$) to a fixed beam. Writing the equation of the total work, the excitation force can be extracted:

$$\begin{aligned} & u_1(0).F(t) = \int_0^1 a(t).\rho_2.S_2.u_2(\breve{x}).\left(\frac{L}{2}.d\breve{x}\right) + \int_{-1}^0 a(t).\rho_1.S_1.u_1(\breve{x}).\left(\frac{L}{2}.d\breve{x}\right) \\ & \Rightarrow F_0 = a_0.\left[\frac{\rho_2.S_2.L}{200}.\left(67 + 17b - \frac{3}{r} + \frac{3b}{r}\right) - \frac{\rho_1.S_1.L}{200}.(-67 + 17b + 3r + 3br)\right] \end{aligned} \quad (17)$$

Once the coefficient *b* is known, the maximum stresses in cylinder 1 and in cylinder 2 are obtained at *x=0* from the following equations:

$$\begin{cases} \sigma_{max\_1} = y_{max}.E_1.\left.\dfrac{\partial\psi}{\partial x}\right|_{x=0} = \left(\dfrac{d_1}{2} + e_1\right).E_1.u_{0,max}.\dfrac{24}{5L^2}(b - br - r - 1) \\ \sigma_{max\_2} = y_{max}.E_2.\left.\dfrac{\partial\psi}{\partial x}\right|_{x=0} = \left(\dfrac{d_2}{2} + e_2\right).E_2.u_{0,max}.\dfrac{24}{5L^2 r}(b - br - r - 1) \end{cases} \quad (18)$$

where $u_{0,max}$ is calculated from equation (2).

In conclusion, with either the single- or the two-body model, the maximum stress in the housing can be calculated analytically as a function of the chosen geometry and the acceleration fixed for the ends.

TRANSFER MATRIX MODEL

This model constitutes an additional step towards a more realistic representation while working with simplified geometries and using formal approaches. Transfer matrices (Zhou, 2000) (Lin, 1969) can be used to represent body and rod as an assembly of embedded cylinders. This method makes it possible to assemble a finite number of cylinders representing the main part of a linear actuator. Another big advantage is that this method allows major local phenomena that influence sizing to be observed and studied.

HYPOTHESIS AND METHODOLOGY

The EMA housing is assumed to be made of embedded cylinders. The first step of the method is to calculate the frequency response of the entire model in response to the forced excitation at its ends. Thus, the mechanical stress can be drawn as a function of the frequency and the first resonant frequency can be determined.

The second step is to study the maximum mechanical stresses in each cylinder for a given frequency (in particular the first resonant frequency) from the values of bending moment and shear force.

The displacement, the rotation, the shear force and the bending moment in each section are calculated with the transfer matrix method, often adopted in the vibratory problems, in particular in acoustics and ultrasonic applications. *U*, *Ψ*, *F* and *T* the transversal, the angular deformation, the shear force and the bending

moment respectively, can be written in a vector of transversal and rotational flow Ω. The vectors of the two ends surfaces of a rod (with fixed cross section S and length L) can be linked with a transfer matrix [Γ]:

$$\begin{pmatrix} U_L \\ \Psi_L \\ F_L \\ T_L \end{pmatrix} = [\Gamma] \begin{pmatrix} U_0 \\ \Psi_0 \\ F_0 \\ T_0 \end{pmatrix} \quad (19)$$

Constituents of transfer matrix [Γ] are developed in appendix B.

The method uses the complex expression of the displacement that is the solution of the wave equation of bending. For each pulsation ω, the magnitude of the displacement is given by equation (3). The quantities Ψ, F, T are calculated from the derivatives of U.

A discretization inside the rod with sections of length x ($x \in [0; L]$) is possible and the vector of flow can be noted:

$$\Omega_i(x) = \begin{pmatrix} U_i(x) \\ \Psi_i(x) \\ F_i(x) \\ T_i(x) \end{pmatrix} \quad (20)$$

Whatever the number of cylinders, a global matrix of the entire assembly can be obtained from the product of the matrices associated with any section. It is then possible to use the boundary conditions at both extremities of the housing to calculate the initial vector $\Omega_1(0)$. Once this initial vector has been determined, each of the other vectors $\Omega_i(x)$ is calculated. This process is repeated for each frequency of excitation. The frequency response of the entire structure can be drawn, choosing the shear force at the extremity as the output. Then, the displacement, the shear force and the bending moment are presented as a function of x in order to calculate the stress in each section of the model, at the resonance frequency.

MATRIX IMPLEMENTATION IN A MODELICA LIBRARY

Modelica models (Mattsson, Elmqvist and Otter, 1998) were elaborated with an object-oriented view that facilitated the study of various arrangements and more localized phenomena, such as viscous friction at the anchorage points. For frequency domain studies, a complex representation was used. To solve this type of dynamic problem, in particular vibratory, acoustic or electronic, the use of standard Modelica libraries enables considering variables and equations using complex numbers (Kûlhnelt, Baüml and Haumer, 2009) (Haumer et al., 2008). Consequently, the tools of the Modelica library created in the laboratory were extended from other types of applications (Otter, 2006) (Olsson et al., 2009). Furthermore, as previously mentioned, object-oriented models targeting critical points in the actuator can be implemented in Modelica language in order to study different candidate designs quickly. The library is made of several types of generic elements which can be combined to model most types of linear actuators. Each element transmits signals of vibrations from a source: acceleration, speed and strength. To simplify and to decrease the number of library components, a generic model source was implemented, including the various inputs for the boundary conditions. The model presented in

FIGURE 7 is an actuator defined as a combination of cylinders. This model is the most complete of the library because it integrates the tools for calculating an assembly of many tubes and useful tools for visualization during the sizing of the housing. The elementary models of beams, stiffness and mass, which can have transverse or rotational displacements, were also implemented to isolate other relevant effects if required.

FIGURE 7 MODELICA/DYMOLA MODELS AND RESULTS OF TRANSFER MATRIX MODEL FOR THE EXAMPLE OF EMA

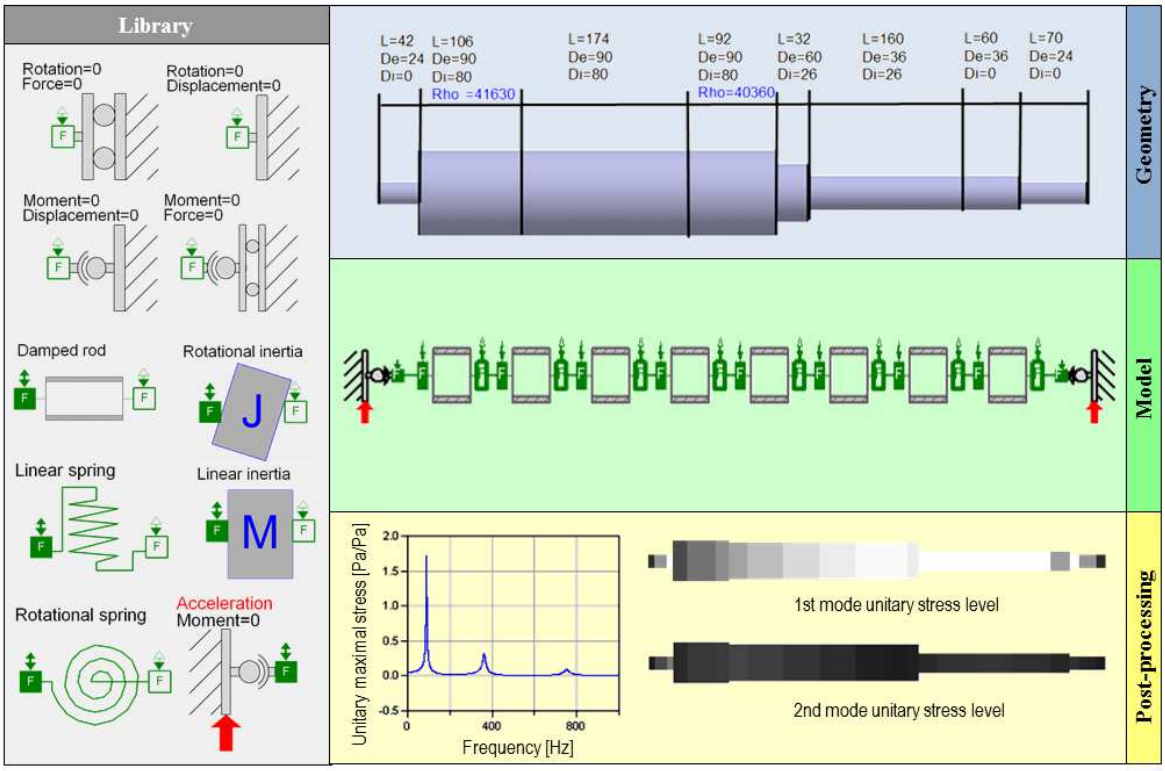

For stress analysis, the first two natural frequencies were studied. They are schematically presented in *FIGURE 1* with an example made of 8 cylinders having dimensions inspired by the EMA of *FIGURE 1 - B*. The cylinders that contain the lumped mass of the internal mechanical parts have a higher density than the one representing the housing since their cross sections do not vary but density has to represent distribution of both masses :

- Based on the model of the actuator, the normed stress (stress divided by admissible stress) response graph is drawn versus frequency.
- To point out the critical zones where these stresses apply, a second tool is introduced to visualize the stress or the displacement of the actuator with the chosen resonant frequency. A better display of the stress locations is provided by dividing each of the cylinders of the model into portions. The resolution is chosen by the designer according to the simulation time constraints. A gray scale is used to represent the qualitative magnitude of stress within the cylinder portions. The lighter the color, the higher the stress. The more numerous the portions of cylinder, the better the localization of dominant effects. When the unitary stress representation shows a totally white zone, the elastic limit of the material has been exceeded.

APPLICATIONS TO DIFFERENT HOUSINGS

In this section, the consistency of the single-body, two-body and realistic model results are shown in *TABLE 1*. Different housing geometries are modeled and compared in *TABLE 2*. Then, for "hybrid" actuators, conclusions are drawn on the influence of the hydraulic fluid and of the mass of the mechanical transmission components.

VALIDATION OF THE THREE MODELLING APPROACHES

Different models were applied to the example of an actuator. For each of those models, stress was calculated for vibration conditions set to a 10 g magnitude considering three different scenarios: only housing mass considered, additional fluid mass (housing full of oil), and vibrations of both components' mass and fluid mass. The dimensions were inspired by one of the real actuators presented in Figure 1.

The results summarized in *TABLE 1* show the global consistency of the methods. It can be seen that the calculated stresses and natural frequency increase when considering a dissymmetric housing is considered while deformation decreases. This can be explained by the fact both equivalent mass and equivalent stiffness increase while the rod (smallest cylinder) stay the same and, therefore, its maximum stress increases. Finally, the inertial effect of the hydraulic fluid is relatively small compared with that of the components of the mechanical transmission. This emphasizes the need to take more additional precautions for the EMA housing than for those of SHA.

Those results have to be compared with the experimental measurements communicated by our industrial partners that gave a first natural frequency of 120Hz while the maximum stress was equal to 1300MPa.

TABLE 1 COMPARISON OF RESULTS FOR DIFFERENT HOUSING MODELING AND CALCULATION METHOD

	Parameters	**Single body**			**Two bodies**		**8 bodies**
		Sinusoidal approach	**Polynomial approach**	**Transfer matrix**	**Polynomial approach**	**Transfer matrix**	**Transfer matrix**
Case	Geometry	Length L=0.74m; diameter d=0.026m; thickness e=0.005m.			Lengths L_1=L_2=0.37m; diameters d_1=0.080m, d_2=0.026m; thicknesses e_1=e_2=0.005m.		Closest to reality.
No additional mass	Maximum displacement (10^{-3}m)	3.5	3.5	3.4	3.4	3.3	2.9
	Maximum stress (MPa)	237	229	237	426	427	502
	1st resonance frequency (Hz)	165	165	164	182	175	187
Additional fluid mass (ρ_h=800kg/m^3)	Maximum displacement (10^{-3}m)	3.9	3.9	3.8	4.3	4.3	3.2
	Maximum stress (MPa)	263	255	263	560	561	567
	1st resonance frequency (Hz)	155	157	156	161	155	177
Additional fluid mass and components mass (4kg)	Maximum displacement (10^{-3}m)	11.6	11.6	11.5	8.8	8.7	6.9
	Maximum stress (MPa)	793	765	926	1146	1225	1254
	1st resonance frequency (Hz)	83	83	82	104	101	122

COMPARISON OF DIFFERENT CURRENT ARCHITECTURES OF EMA HOUSINGS

In the preliminary phase, choices have to be made in order to define the actuator architecture and its housing geometry, assessing different candidate solutions. To illustrate these studies, the different cases for a standard geometry of actuator housing, presented in *FIGURE 1*, were compared, under the following assumptions:

- Components of mechanical power transmission are not considered in the calculation of equivalent stiffness but have an influence on the equivalent mass.
- In the same way, the hydraulic fluid does not influence the equivalent stiffness yet it has an influence on the mass through its density of ρ_h=800 kg/m^3.
- Test conditions are the same for all cases: 10 g acceleration and quality coefficient equal to 30.

TABLE 2 COMPARISON OF CALCULATED STRESS AND FIRST FREQUENCY FOR STANDARD ACTUATOR HOUSING GEOMETRY

Comparison	**Standard model**	**Theoretical maximum stress (MPa)**		**Theoretical frequency (Hz)**	**Theoretical maximum displacement (10^{-3} m)**
		Polynomial approach	Transfer matrix		
Hydraulic / EMA	EMA 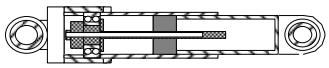	349	367	179	3.1
	EMA 	**1178**	**1310**	73	15.8
	EHA 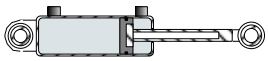	181	188	280	1.1
Long / Short actuator	Long EMA 	**1178**	**1310**	73	15.8
	Short EMA 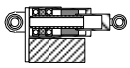	161	180	660	0.2
Large / Small diameter	EBMA1 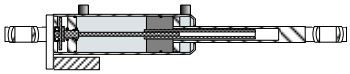	**1146**	**1254**	122	6.9
	EBMA2 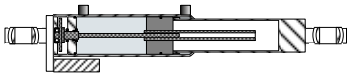	209	238	256	1.3

These results suggest the following conclusions:

- The maximum stresses and the displacement are greater in EMA than in SHA. Moreover, these stresses are close to the elastic limit of the material or even greater in some cases. Thus, vibration induced stress is a sizing factor for EMA whereas in hydraulic actuators, it remains low in comparison with pressure-induced stress. This comes from the added mass of components of the mechanical power transmission, which strongly impacts mechanical stresses.
- Stresses are directly related to the length of the actuator. Compact actuators are stiffer than long actuators which, consequently, have a higher maximum displacement and induced stress.

- Increasing diameter strongly decreases the maximum stress and the displacement of the housing. To design actuator housings, it is better to choose large diameter rather than large thickness as long as the actuator fits into the on-board compartment.

Concerning the methods, the mean simulation time required to generate these outputs is greater for transfer matrix method than for the two-body method. They both give similar results with good accuracy compared with experimental results. But the transfer matrix method necessitates good knowledge of the housing geometry which is often not available at the preliminary design phase. Therefore, it can be concluded that the two-body model is a sufficiently good approximation to calculate the housing stress early on and efficiently.

EXPLORATION DESIGN OF EMA HOUSINGS

In the aim of comparing and making choices for actuator housing geometry early in design phases, a rapid design exploration of housings is very useful. Nevertheless at preliminary sizing level, components geometries and mass, useful for housing design, are not fully specified although they can be roughly scaled considering the mission profile's sizing criterion.

DESIGN EXPLORATION OF SINGLE-BODY MODEL

If we consider the single body equations (6;7;9) for the housing, under the assumption of small thickness with regard to diameter and a large additional mass, it is possible to say that for small changes in the thickness, diameter and length, the equivalent mass and stiffness become proportional to:

$$M_{eq} \propto cste, \; K_{eq} \propto \frac{e.d^3}{L^3} \tag{21}$$

Furthermore, under these same assumptions, the variations of the housing mass, the maximum constraint and the first natural frequency can be expressed:

$$M \propto e.d.L, \; \sigma_{\max} \propto \frac{L}{e.d^2}, \; f_0 \propto \sqrt{\frac{e.d^3}{L^3}} \tag{22}$$

This means that, to lower the stress, it is more interesting to increase the diameter than to increase the thickness. Equations (21; 22) also mean that the length has a huge effect on the stress and natural frequency.

Now, if the assumptions change and there is no additional mass or this mass is negligible with regard to the housing equivalent mass, the equivalent mass is now proportional to:

$$M_{eq} \propto e.d.L \tag{23}$$

and the variations of the maximum constraint and the first natural frequency become:

$$\sigma_{\max} \propto \frac{L^2}{d}, \; f_0 \propto \frac{d}{L^2} \tag{24}$$

Here, the thickness has hardly any effect on the stress or natural frequency and the length has more effect than the diameter.

Globally, it is observed that frequencies decrease while maximum stress increases when the actuator length increases. That is why, in aerospace applications, particular attention has to be paid to long housings having their first mode in the excitation frequency range. Concerning EMA housing, it seems more efficient to

choose higher diameters than thicknesses design to decrease internal maximum stress. For the multiple-body model, it is not so easy to study the effect of diameter or thickness variations.

DESIGN EXPLORATION OF TWO-BODY MODEL

As described in (Budinger et al., 2012) (Maré, 2011), the mass and geometry of a roller-screw technology can be estimated considering either the maximum force or the fatigue force applied to it but also the stroke needed for the application. Taking maximum force F_{max} and stroke Δx as definition parameters, nut diameter d_{nut}, nut mass M_{nut}, screw diameter d_{screw} and screw mass M_{screw} can be estimated using scaling laws:

$$d_{nut} \propto F_{\max}^{1/2},\ M_{nut} \propto F_{\max}^{3/2},\ d_{screw} \propto F_{\max}^{1/2},\ M_{screw} \propto F_{\max}.\Delta x \quad (25)$$

For all other components the process is the same but most of the time only the roller-screw component is important for housing vibrations sizing. The reason is that the roller-screw mass has a huge impact on the kinetic energy and the equivalent mass because of its location (in the middle of the actuator, where displacement magnitude is maximum). This additional embedded mass is not directly the roller-screw mass since the whole screw mass is not centered but is considered to be homogeneously distributed along the actuator like the fluid in equation (9):

$$M_{comp} = 2.M_{screw}/\pi + M_{nut} \quad (26)$$

It will be considered that the mounting of the screw nut or the thrust bearing allows some rotational degrees of freedom like as for a ball joint. Thus mechanical components do not have an impact on the equivalent stiffness.

Concerning integration parameters, parallel axis architecture will be chosen (as in *FIGURE 1 A-E*). For such architecture, the inner diameters of the housing are limited by the roller-screw geometry (*FIGURE 8*):

$$d_2 \geq d_{screw},\ d_1 \geq d_{nut} + 2.e_2 \quad (27)$$

To simplify the design exploration, and even if the solution can be improved, equations (27) become:

$$d_2 = d_{nut},\ d_1 = d_2 + 2.e_2 \quad (28)$$

FIGURE 8 HOUSING GEOMETRY ASSUMPTIONS

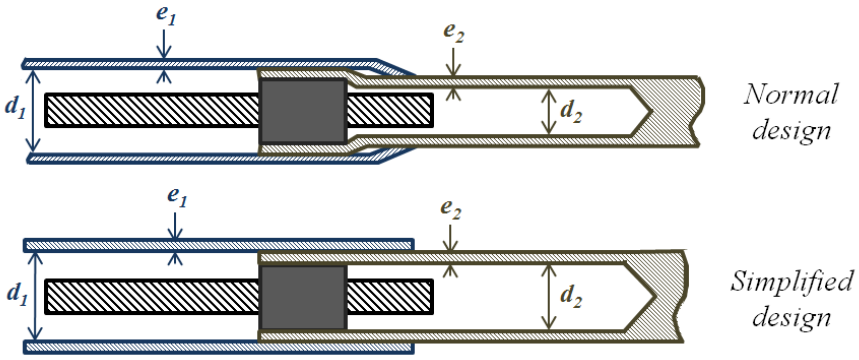

The two-body method needs L_{max} the extended length of the actuator, as an input for calculation and this parameter is proportional to the useful stroke:

$$L_{\max} \propto \Delta x \quad (29)$$

Making the assumption of a simplified housing design and using the relations described in equations (25; 26; 29), it is possible to fix the thickness values in order to minimize mass without exceeding the admissible stress under vibration conditions (*FIGURE 9*).

FIGURE 9 DESIGN EXPLORATION OF THE ACTUATOR MASS FOR DIFFERENT MISSION PROFILE FEATURES

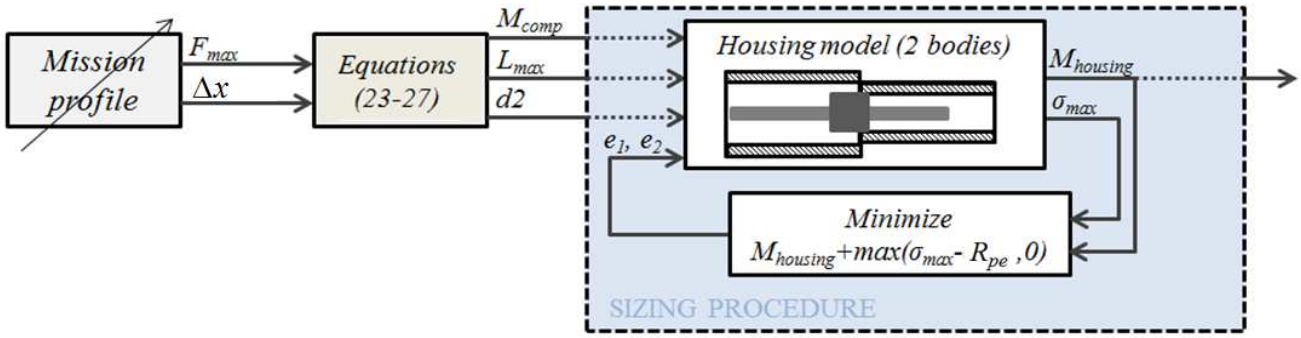

Calculations were done for a 10 g acceleration magnitude and a quality factor of $Q=30$. The calculation method used was the two-body model with the polynomial deformation. Housing was planned be made of low alloyed steel with a maximum elastic shearing stress of R_e=700MPa, a Young's modulus of E=210GPa and a density of ρ=7800kg/m^3. Considering some radius of curvature on the geometry, stress concentration may appear. In addition to that, the embedded mass was an estimation of the real roller-screw mass. Therefore a safety factor of 2 was taken and the calculated stress was not allowed to exceed R_{pe}=350MPa.

The calculated housing mass is presented in

FIGURE 10 and *FIGURE 11* according to the nut diameter and the extended length of the actuator. The equivalent mass was firstly set equal to the embedded component mass alone (*FIGURE 11-A*) and then the housing inertia was added (

FIGURE 10-*B*) to compare the two effects.

These figures give rise to some important remarks:

- For a short length, vibration is not the sizing criterion and housing geometry depends on mechanical parts integration and consequently on the maximum force.
- When the length increases, the two mass effects (body and embedded components masses) combine in a nonlinear way.
- For a small diameter, the increase of the mass is strongly dependent on the housing length.
- For a long actuator, the rod stress reaches admissible stress limits; it appears that an optimal diameter can be found to reduce housing weight. This suggests that an optimization loop should be implemented taking flexibility on the values of d_1 and d_2 into account.

FIGURE 10 HOUSING MASS ACCORDING TO THE EXTENDED LENGTH AND THE NUT DIAMETER

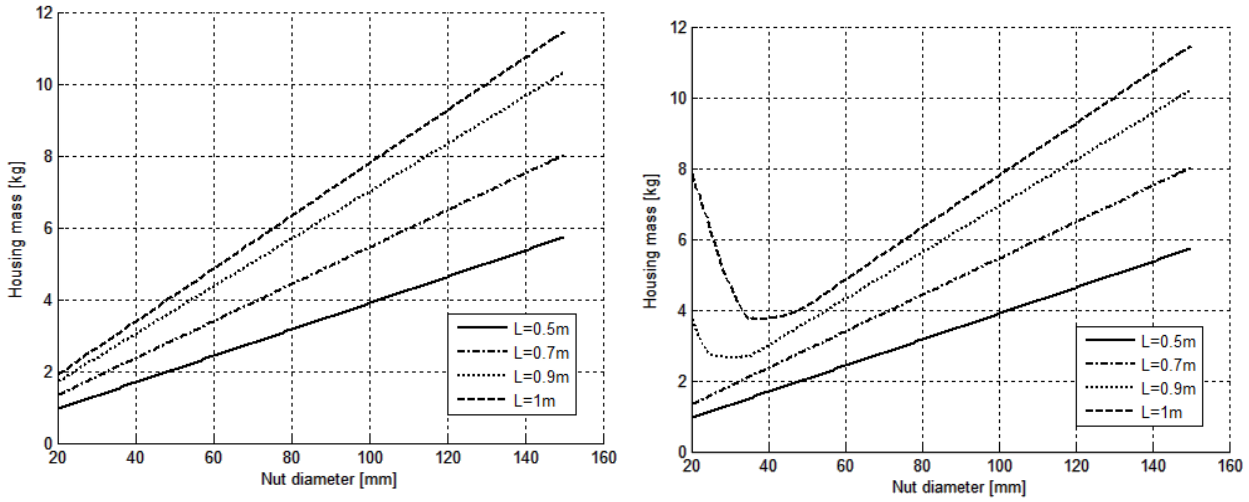

A – Housing density is zero *B – Both housing and components masses are considered*

FIGURE 11 OPTIMAL DIAMETER DETECTION VS. EXTENDED LENGTH INCREASE

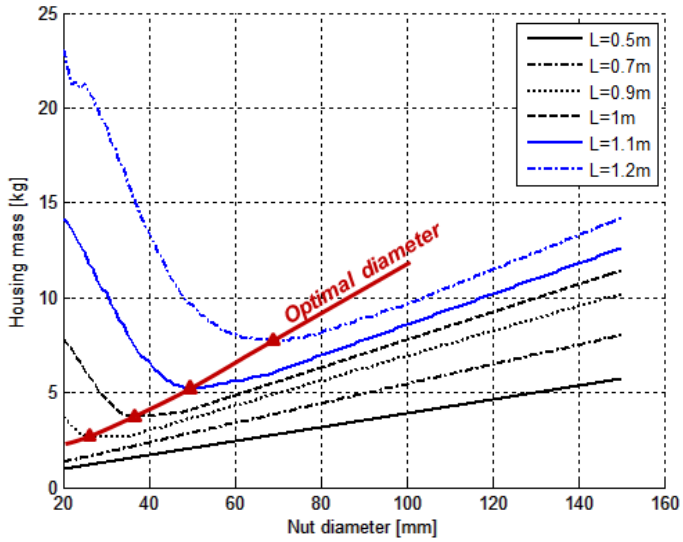

CONCLUSION

A methodology and associated models have been proposed in this article which could accelerate the preliminary design phase by providing fast and efficient means of sizing actuators housings in a vibratory environment. After studying housing stresses in a linear actuator, the impact of the harsh aerospace vibratory environment was studied with different representations of the actuator housing. Three analytical models were proposed and compared: one considering a single-body for the housing, a second one based on a two-body housing and the third a more realistic one with multi-body transfer matrix modeling. Of these three methods, the second one appeared to provide the best trade-off between calculation time and precision of results, the transfer matrix approach remaining the best way to localize the critical stress zone for variable geometry and mass distribution. Comparisons between standard linear actuator geometries were used to explore different housing topologies. The models studied showed that vibrations were a key sizing criterion for long EMA

(Electro Mechanical Actuator) housing but not for SHA (Servo Hydraulic Actuator) housing (mostly sized by the internal pressure strength). This is why such sizing tools are useful for EMA design, which embeds more mechanical components, strongly increasing modal mass and inducing strong vibrations. Some exploratory studies on the housing geometry were performed to highlight the compromise between diameter, thickness and extended length in vibration design.

Acknowledgment

Most of the research leading to these results has received funding from the European Union Seventh Framework Program (FP7/2007- 2013) "ACTUATION 2015: Modular Electro Mechanical Actuators for ACARE 2020 Aircraft and Helicopters" under grant agreement n° 284915.

Appendix A: two-body model expressions

$$M_{eq} = \alpha_1 . b^2 + \beta_1 . b + \gamma_1$$

with:

$$\begin{cases} \alpha_1 = \dfrac{\rho_1 S_1 L}{2} \dfrac{(1113 + 399.r + 38.r^2)}{31500} + \dfrac{\rho_2 S_2 L}{2} \dfrac{(38 + 399.r + 1113.r^2)}{31500.r^2} \\ \beta_1 = \dfrac{\rho_1 S_1 L}{2} \dfrac{(-7686 - 840.r + 76.r^2)}{31500} + \dfrac{\rho_2 S_2 L}{2} \dfrac{(-76 + 840.r + 7686.r^2)}{31500.r^2} \\ \gamma_1 = \dfrac{\rho_1 S_1 L}{2} \dfrac{(17073 - 1239.r + 38.r^2)}{31500} + \dfrac{\rho_2 S_2 L}{2} \dfrac{(38 - 1239.r + 17073.r^2)}{31500.r^2} \end{cases}$$

$$K_{eq} = \alpha_2 . b^2 + \beta_2 . b + \gamma_2$$

with:

$$\begin{cases} \alpha_2 = \dfrac{8.E_1 I_1}{L^3} \dfrac{(456 + 108.r + 36.r^2)}{125} + \dfrac{8.E_2 I_2}{L^3} \dfrac{(36 + 108.r + 456.r^2)}{125.r^2} \\ \beta_2 = \dfrac{8.E_1 I_1}{L^3} \dfrac{(-912 + 72.r^2)}{125} + \dfrac{8.E_2 I_2}{L^3} \dfrac{(-72 + 912.r^2)}{125.r^2} \\ \gamma_2 = \dfrac{8.E_1 I_1}{L^3} \dfrac{(456 - 108.r + 36.r^2)}{125} + \dfrac{8.E_2 I_2}{L^3} \dfrac{(36 - 108.r + 456.r^2)}{125.r^2} \end{cases}$$

APPENDIX B: transfer matrix expressions

$c = E\left(1 + \dfrac{j}{Q}\right)$ is the complex form of Young Modulus.

$G = \dfrac{c}{2(1+\nu)}$ is the shear modulus, ν the Poisson coefficient.

$S = \dfrac{\pi}{4}\left(d_{ext}^2 - d_{\text{int}}^2\right)$ is the cross-section area.

$J = \frac{\pi}{64}\left(d_{ext}^4 - d_{\text{int}}^4\right)$ is the quadratic moment.

$a = \frac{3}{4}\frac{\left(d_{ext}^2 + d_{\text{int}}^2\right)\left(d_{ext} - d_{\text{int}}\right)}{\left(d_{ext}^3 - d_{\text{int}}^3\right)}$ is the Timoshenko coefficient.

$$[\Gamma]=\begin{pmatrix} \frac{\alpha_M ch(k_2L)-\beta_M cos(k_1L)}{\alpha_M-\beta_M} & \frac{\alpha_T sh(k_2L)-\beta_T sin(k_1L)}{\beta_\psi\alpha_T-\alpha_\psi\beta_T} & \frac{\beta_\psi sin(k_1L)-\alpha_\psi sh(k_2L)}{\beta_\psi\alpha_T-\alpha_\psi\beta_T} & \frac{cos(k_1L)-ch(k_2L)}{\alpha_M-\beta_M} \\ \frac{\beta_\psi\alpha_M sh(k_2L)+\alpha_\psi\beta_M sin(k_1L)}{\alpha_M-\beta_M} & \frac{\beta_\psi\alpha_T ch(k_2L)-\alpha_\psi\beta_T cos(k_1L)}{\beta_\psi\alpha_T-\alpha_\psi\beta_T} & \frac{\alpha_\psi\beta_\psi cos(k_1L)-\alpha_\psi\beta_\psi ch(k_2L)}{\beta_\psi\alpha_T-\alpha_\psi\beta_T} & -\frac{\beta_\psi sh(k_2L)+\alpha_\psi sin(k_1L)}{\alpha_M-\beta_M} \\ \frac{\beta_T\alpha_M sh(k_2L)+\alpha_T\beta_M sin(k_1L)}{\alpha_M-\beta_M} & \frac{\beta_T\alpha_T ch(k_2L)-\alpha_T\beta_T cos(k_1L)}{\beta_\psi\alpha_T-\alpha_\psi\beta_T} & \frac{\alpha_T\beta_\psi cos(k_1L)-\alpha_\psi\beta_T ch(k_2L)}{\beta_\psi\alpha_T-\alpha_\psi\beta_T} & -\frac{\beta_T sh(k_2L)+\alpha_T sin(k_1L)}{\alpha_M-\beta_M} \\ \frac{\beta_M\alpha_M ch(k_2L)-\alpha_M\beta_M cos(k_1L)}{\alpha_M-\beta_M} & \frac{\beta_M\alpha_T sh(k_2L)-\alpha_M\beta_T sin(k_1L)}{\beta_\psi\alpha_T-\alpha_\psi\beta_T} & \frac{\alpha_M\beta_\psi sin(k_1L)-\beta_M\alpha_\psi sh(k_2L)}{\beta_\psi\alpha_T-\alpha_\psi\beta_T} & \frac{\alpha_M cos(k_1L)-\beta_M ch(k_2L)}{\alpha_M-\beta_M} \end{pmatrix}$$

with:

$$k_1 = \sqrt{\frac{\sqrt{\rho J\left(1+\frac{c}{aG}\right)\omega_i^2 + 4cJ\rho S\omega_i^2\left(1-\frac{\rho J\omega_i^2}{aSG}\right)} + \rho J\left(1+\frac{c}{aG}\right)\omega_i^2}{2c\,J}}\ ;$$

$$k_2 = \sqrt{\frac{\sqrt{\rho J\left(1+\frac{c}{aG}\right)\omega_i^2 + 4cJ\rho S\omega_i^2\left(1-\frac{\rho J\omega_i^2}{aSG}\right)} - \rho J\left(1+\frac{c}{aG}\right)\omega_i^2}{2cJ}}\ ;$$

$\alpha_M = cJ\left(\frac{\rho\omega_i^2}{aG} - k_1^2\right)$; $\beta_M = cJ\left(\frac{\rho\omega_i^2}{aG} + k_2^2\right)$; $\alpha_\psi = \frac{k_1(\alpha_M + aSG)}{aSG - \rho\omega_i^2 J}$; $\beta_\psi = \frac{k_2(\beta_M + aSG)}{aSG - \rho\omega_i^2 J}$; $\alpha_T = \frac{\alpha_\psi - k_1}{aSG}$; $\beta_T = \frac{\beta_\psi - k_2}{aSG}$

NOMENCLATURE

CAE	=	Computer Aided Engineering
EBMA	=	Electrical Back-up Mechanical Actuator
EBHA	=	Electrical Back-up Hydraulic Actuator
EHA	=	Electro-Hydrostatic Actuator
EMA	=	Electro-Mechanical Actuator
FEM	=	Finite Element Method
PbW	=	Power-by-Wire
SHA	=	Servo Hydraulic Actuator
TVC	=	Thrust Vector Control

REFERENCES

Agency, E.A.S. (2007) *Certification Specifications and Acceptable Means of Compliance for Large Aeroplanes CS-25*.

Boubet, R. (1998) 'Fonction Carter', *Techniques de l'Ingénieur*, vol. BM5175.

Budinger, M., Liscouet, J., Hospital, F. and Maré, J.C. (2012) 'Estimation Models for the Preliminary Design of Electro-Mechanical Actuators', *Proceedings of IMechE, Part G: Journal of Aerospace Engineering*, vol. Vol. 226, pp. pp. 243-259.

Chevalier, P.Y., Grac, S. and Liegois, P.Y. (2010) 'More electrical landing gear actuation systems', 2010 Recent Advances in Aerospace Actuation Systems and Components, Toulouse, France, May 5-7 2010.

Cowan, J.R. and Weir, R.A. (1993) 'Design and test of electromechanical actuators for thrust vector control', The 27th Aerospace Mechanisms Symposium, NASA Ames research center, CA - USA, May 12-14 1993, pp. 349-366.

Davis, M.A. (1984) 'High performance electromechanical servoactuation using brushless DC motors', Technical bulletin 150, MOTOR-CON '84 Conference, Atlantic City, April 1984.

Dée, G., Vanthuyne, T. and Alexandre, P. (2010) 'An electrical thrust vector control system with dynamic force feedback', 2010 International Conference on Recent Advances in Aerospace Actuation Systems and Components, Toulouse, Jun. 13-15 2010, pp. 75-79.

EUROCAE (2005) *DO160E – Environmental conditions and test procedures for airborne equipment (ED-14E)*.

Gerardin, M. and Rixen, D. (1993) *Théorie des vibrations*.

Grand, S. and Valembois, J.M. (2004) 'Electromechanical actuators design for thrust vector control', 3rd International conference on R3ASC, Toulouse, France, 24-26 Nov. 2004.

Harris, C.M. and Piersol, A.G. (2001) *Harris'shock and vibration handbook*, New York, McGraw-Hill.

Hatch, M.R. (2001) *Vibration Simulation Using MATLAB and ANSYS*, Chapman & Hall/CRC.

Haumer, A., Kral, C., Gragger, J.V. and Kapeller, H. (2008) 'Quasi-stationary modeling and simulation of electrical circuits using complex phasors', Modelica Conference, Mar. 3-4 2008.

INCOSE (2004) *Systems engineering handbook,* INCOSE Technical Product.

Jensen, S.C., Jenney, G.D. and Dawson, D. (2000) 'Flight test experience with an electromechanical actuator on the F-18 systems research aircraft', The 19th Digital Avionics Systems Conferences, Philadelphia, PA - USA, Oct. 7-13 2000.

Karam, W. and Maré, J.C. (2006) 'Comparison of EMA and HA performance for dynamic load simulators', Proc. Bath Power Transmission and Motion Control Symposium - PTMC 2006, Bath, England, Sept. 7-9 2006, pp. 211-224.

Kûlhnelt, H., Baüml, T. and Haumer, A. (2009) 'SoundDuctFlow: A Modelica library for modeling acoustics and flow in duct networks', 7th Modelica Conference, Como, Italy, Sept. 20-22 2009.

Lagrange, J.L. (1853) *Mécanique analytique, Tome 1*.

Lin, Y.K. (1969) 'A brief survey of transfer matrix techniques with special reference to the analysis of aircraft planes', *Journal of Sound Vibrations*, vol. 10 (1), pp. pp. 103-143.

Liscouet, J., Budinger, M., Maré, J.C. and Orieux, S. (2011) 'Modelling approach for the Simulation-Based Preliminary Design of Power Transmissions', *Mechanism and Machine Theory*, vol. Vol. 46, n° 3, pp. pp. 276-289.

Maré, J.C. (2011) 'Combining hydraulics and electrics for innovation and performance improvement in aerospace actuation', Proceedings of the Twelfth Scandinavian International Conference on Fluid Power, Tampere, Finland, May 18-20 2011.

Mattsson, S.E., Elmqvist, H. and Otter, M. (1998) 'Physical system modeling with Modelica', *Control Engineering Practice*, vol. 6, pp. pp. 501-510.

Morgado, T.L.M., Branco, C.M. and Infante, V. (2008) 'A failure study of housing of the gearboxes of series 2600 locomotives of the Portuguese Railway Company', *Engineering Failure Analysis*, vol. 15, pp. pp.154-164.

Olsson, H., Otter, M., Elmqvist, H. and Brück, D. (2009) 'Operator overloading in Modelica 3.1', 7th Modelica Conference, Como, Italy, Sept. 20-22 2009.

Otter, M. (2006) 'The Linear Systems library for continuous and discrete control systems', Modelica Conference, Sept. 4-5 2006.

Rebbechi, B. (1999) 'Active control of gearbox vibration', ACTIVE 99, Fort Lauderdale, Florida, USA, Dec. 2-4 1999.

Samuelson, J., Holm, D. and Esping, B. (1991) 'Optimisation of fatigue resistance of a hydraulic cylinder housing', *Materials & Design, Elsevier*, vol. Vol.13, Nb.3, 1991, pp.141-157., pp. pp.141-157.

Todeschi, M. (2010) 'Airbus – EMAs for flight actuation systems – perspectives', 2010 International Conference on Recent Advances in Aerospace Actuation Systems and Components, Toulouse, France, Jun. 13-15 2010, pp. 1-8.

Topaç, M.M., Günal, H. and Kuralay, N.S. (2009) 'Fatigue failure prediction of a rear axle housing prototype by using finite element analysis,', *Engineering Failure Analysis*, vol. 16, pp. pp.1474-1482.

Van den Bossche, D. (2001) 'A380 primary flight control actuation system', 2001 International Conference on Recent Advances in Aerospace Actuation Systems and Components, Toulouse, France, Jun. 13-15 2001, pp. 1-4.

Vanthuyne, T. (2009) 'An electrical thrust control vector system for the VEGA launcher', 13th European Space Mechanisms and Tribology Symposium – ESMATS 2009, Vienna, Austria, Sept. 23–25 2009.

Zhou, G. (2000) 'The performance and design of ultrasonic vibration system for flexural mode', *Ultrasonics*, vol. vol. 38, pp. pp. 979-984.

CORRESPONDING AUTHOR

Marc Budinger can be contacted at: marc.budinger@insa-toulouse.fr